Pharmacogn. Mag.
A multifaceted peer reviewed journal in the field of Pharmacognosy and Natural Products
www.phcog.com | www.phcog.net

ORIGINAL ARTICLE

Synthesis, Characterization, and Anti-hepatocellular Carcinoma Effect of Glycyrrhizin-coupled Bovine Serum Albumin-loaded Luteolin Nanoparticles

Yongxia Yang, Huaguo Liang[1], Pei Zeng, Wei Fu[1], Jingwei Yu[1], Luxi Chen[1], Dong Chai[1], Ying Wen[1], Ali Chen[2], Yongli Zhang[1]

Department of Electronic Information Engineering, School of Medical Information Engineering, [1]Department of Cell Biology and Medical Genetics, School of Life Sciences and Biopharmaceutics, [2]The Experiment Centre, School of Chemistry and Chemical Engineering, Guangdong Pharmaceutical University, Guangzhou 510006, P. R. China

Submitted: 19-Jan-2021 Revised:29-Apr-2021 Accepted: 14-Oct-2021 Published: 28-Mar-2022

ABSTRACT

Background: Luteolin (Lut) is a natural flavonoid with low water solubility. Many studies have revealed that its antitumor effect is more understandable. **Objectives:** Synthesis of glycyrrhizin-coupled bovine serum albumin-loaded Lut nanoparticles (GL-BSA-Lut-Nps) to progress the water solubility, anticancer effect, liver targeting, cycle arrest, induction apoptosis, and regulating the metabolism of Lut. **Materials and Methods:** The activity screening of GL-BSA-Lut-Nps on Hepatocellular Carcinoma Bel-7402 cells was spotted by 3-(4,5-dimethyl-2-thiazolyl)-2,5-diphenyl-tetrazolium bromide (MTT) assay, cell cycle, and apoptosis were measured by flow cytometry. The solubility of GL-BSA-Lut-Nps was evaluated by ultraviolet spectrophotometer. Fluorescein isothiocyanate was employed to label the drug, and the fluorescence intensity of cells after drug uptake was detected under a fluorescence microscope to sense the targeting of GL-BSA-Lut-Nps to tumor cells. The differences of metabolites between Bel-7402 cells treated with GL-BSA-Lut-Nps and the control group were considered by 1 hydrogen-nuclear magnetic resonance metabolomics. **Results:** The results presented that the GL-BSA-Lut-Nps prepared by solvent removal method had good anti-tumor activity and water solubility *in vitro* and the No. 4 Lut nanoparticles (GL-BSA-Lut-Nps-4) screened by the MTT method had the best effect. The IC_{50} of the GL-BSA-Lut-Nps-4 on the Bel-7402 cell inhibition test was 1.999 ± 0.880 mg/mL. The results of cell cycle and apoptosis displayed that the anticancer effect of the prescription is more palpable. The results of the fluorescence original method are proposed to confirm that the experimentally created GL-BSA-Lut-Nps-4 have a liver targeting effect. The study of metabolomics further clarified the metabolic regulation effect of GL-BSA-Lut-Nps-4 on Bel-7402 cells. **Conclusion:** It delivers a theoretical basis for the development of new high-efficiency and low-toxicity traditional Chinese medicine preparations for liver cancer.

Key words: 1 hydrogen-nuclear magnetic resonance, Bel-7402, hepatocellular carcinoma, luteolin, metabolomics, nanoparticles

SUMMARY

- This study assembled Lut-GL nanoparticles mediated by albumin, which augmented the water solubility, targeting, and anti-hepatoma effect of Lut.
- Characterization studies, thermal gravimetric and differential scanning calorimetry analysis, established that Lut was effectively encapsulated with nanocarriers, and the structure of Glycyrrhizin-coupled bovine serum albumin-loaded luteolin nanoparticles-4 was stable.

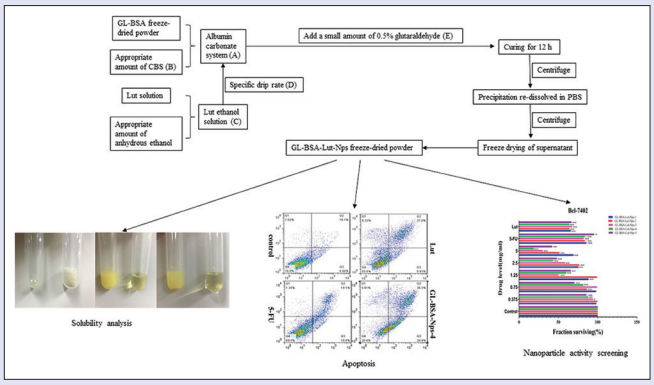

Abbreviations used: HCC: Hepatocellular Carcinoma; Lut: Luteolin; BSA: Bovine serum albumin; GL: Glycyrrhizin; GL-BSA-Lut-Nps: Glycyrrhizin-coupled bovine serum albumin-loaded luteolin nanoparticles; MTT: 3-(4,5-dimethyl-2-thiazolyl)-2,5-diphenyl-tetrazolium bromide; FITC: Fluorescein isothiocyanate; DMSO: Dimethyl sulfoxide; DMEM: Dulbecco's modified eagle medium; FBS: Fetal bovine serum; 5-FU: 5-Fluorouracil; PI: Propidium iodide; CBS: Carbonate buffer solution; PBS: Phosphate buffer solution; ^{1}H NMR: 1 hydrogen-nuclear magnetic resonance; TG: Thermal gravimetric; DSC: Differential scanning calorimeter; UV: Ultraviolet; PCA: Principal components analysis.

Correspondence:

Dr. Yongli Zhang,
Department of Cell Biology and Medical Genetics, School of Life Sciences and Biopharmaceutics, Guangdong Pharmaceutical University, Guangzhou Key Laboratory of Construction and Application of New Drug Screening Model Systems, 280 Wai Huan Dong Road, University City of Guangzhou, Guangzhou 510006, Guangdong, China.
E-mail: zyl28_gdpu@163.com

DOI: 10.4103/pm.pm_34_21

Access this article online
Website: www.phcog.com
Quick Response Code:

INTRODUCTION

Liver cancer is one of the most communal cancers in our country, it is also one of the foremost causes of cancer deaths.[1] By far the most common cancer of the liver is Hepatocellular carcinoma (HCC) in chief liver cancer.[2,3] The existing treatment methods are traditional,

Cite this article as: Yang Y, Liang H, Zeng P, Fu W, Yu J, Chen L, *et al*. Synthesis, characterization, and anti-hepatocellular carcinoma effect of glycyrrhizin-coupled bovine serum albumin-loaded luteolin nanoparticles. Phcog Mag 2022;18:216-25.

toxic and have side effects.[4,5] Treatment of cancer using traditional Chinese medicine or drugs with minor side effects and good targeting has become a drift.[6]

In current years, more and more studies have been directed on the anti-tumor effects of luteolin (Lut). Lut is a low water-soluble natural flavonoid compound, which is found in many natural herbs and fruits.[7] Studies at home and overseas have found that Lut has an obvious inhibitory effect on a diversity of solid tumors,[8-10] and that Lut has anti-tumor cell proliferation, anti-inflammation, anti-oxidation, induction of autophagy, and apoptosis.[11,12] However, the anti-tumor function of Lut is more embattled and multi-level and it can unswervingly act on tumor cells, inhibit with cell metabolism.[13] It can also act on the body tissue, improve the body immunity, inhibit the formation of blood vessels in tumor tissue,[14] recover the sensitivity of tumor cells to radiotherapy and chemotherapy, inhibit the metastasis and invasion ability of tumor.[15,16] Albumin upholds plasma osmotic pressure and plays an essential role in endogenous material transport.[17] Albumin is biodegradable and the product is inoffensive to the human body and the preparation of albumin nanoparticles is possible.[18] Albumin nanoparticles have active targeting effect and are relaxed to be concentrated in tumor tissues, which can improve the bioavailability of drugs and decrease the toxic and side effects of free drugs.[19] The bovine serum albumin (BSA) is the most usually employed drug carrier protein. Because of its wide source, easy extraction and low cost, BSA has developed one of the most commonly used proteins to study the interaction between bioactive small molecules and proteins.[20] Glycyrrhizin (GL) fits to pentacyclic triterpene soap and is the most vital active ingredient in liquorice. It has the functions of anti-inflammation, augmenting immunity, and inhibiting the growth of cancer cells. GL can be expended in large quantities in the liver because the liver cell surface has GL receptors, which can be extremely uttered in tumor cells when liver cancer occurs.[21] GL molecules are coupled to the surface of BSA and the GL-BSA is gained as drug carriers. The active targeting is mainly reproduced in the specific binding of GL to liver surface receptors and the active enrichment of liver sites.[22] Our research group created albumin-mediated GL nanoparticles of Lut in the primary stage and studied the dosage formulation of the drug, so as to surge its water solubility and improve the targeting capability on liver cancer cells and its anti-liver cancer effect. Lut nanoparticles have brilliant solubility in drug purity, saturation solubility, dissolution rate and bioavailability.[23]

In this study, Glycyrrhizin-coupled bovine serum albumin-loaded luteolin nanoparticles (GL-BSA-Lut-Nps) comprising GL coupled with BSA were prepared by solvent removal method and the solid monomer of these GL-BSA-Lut-Nps was effectively coated. The results of the solubility test of Lut the preparation GL-BSA-Lut-Nps powder displayed that the preparation of drug dosage form was scientific and practicable. In this experiment, 3-(4,5-dimethyl-2-thiazolyl)-2,5-diphenyl-tetrazolium bromide (MTT) assay was employed to prove the anti-tumor efficacy of preparing GL-BSA-Lut-Nps and to screen the most activity of the nanoparticles and to conduct follow-up anti-tumor drug research for the screening GL-BSA-Lut-Nps-4. According to the earlier research results of our group, Lut has a good anti-tumor biological activity and endorses cell apoptosis by inducing autophagy in the HCC HepG2 cells.[24] Therefore, we took Lut as the subject for the alteration of nanoparticles. Cell cycle and apoptosis studies check the biological behavior of GL-BSA-Lut-Nps-4 against tumors. Fluorescence *in situ* hybridization experiment was employed to measure the targeting of GL-BSA-Lut-Nps-4 on liver cancer cells for active targeted therapy. The metabolomics study of Bel-7402 cells was conducted to confirm whether the anti-tumor effect of GL-BSA-Lut-Nps-4 was reliable with the biological level *in vitro* and at the level of downstream metabolite group, so disclose the molecular mechanism of GL-BSA-Lut-Nps-4's anti-liver cancer effect at the downstream level of metabolite group and explain the metabolite target and molecular marker of its action. By comparing the results of the above studies on GL-BSA-Lut-Nps-4 and Lut at the cellular level, this study purposes to expose whether our GL-BSA-Lut-Nps-4 dosage form is greater in terms of research. This study intentions to play an experimental foundation for the construction of new Chinese medicine drugs against liver cancer with high competence and low toxicity.

MATERIALS AND METHODS

Materials

HCC cells (Bel-7402), human cervical cancer cells (Hela), and colon cancer cells (HCT8) were attained from the Institute of Biochemistry and Cell Biology, CAS (Shanghai, China). Glycyrrhizic acid powder, Fluorescein isothiocyanate (FITC), and Lut were bought from Zuoke Biotechnology Development Co., Ltd. (Guangzhou, China). Methanol was provided by Merck Group (Germany). BSA, dialysis bag, phosphate buffer solution (PBS), Dimethyl sulfoxide (DMSO) and 6-well plates, 96-well plates, 50 cm^2 culture dishes, 0.5% glutaraldehyde was obtained from Suyan Biological Technology Co., Ltd. (Guangzhou, China). Dulbecco's modified eagle medium (DMEM) High Glucose Medium, 10% fetal bovine serum, and 0.25% trypsin was purchased from GIBCO Co. (USA). 5-FU was expanded from The First Affiliated Hospital of Guangdong Pharmaceutical University (Guangzhou, China). Apoptosis Detection Kit was bought from Nanjing Kaiji Biological Technology Development Co., Ltd. (Nanjing, China). D_2O was procured from Qingdao Tenglong Technology Co., Ltd. (Qingdao, China). All reagents and chemicals were assimilated and employed as received according to manufacturers' instructions if without superior explained.

Preparation of glycyrrhizin-bovine serum albumin freeze-dried powder

The accurate weighing 180.0 mg glycyrrhizic acid powder was added into 12 mL methanol (prepared in advance), and the mixture was stimulated evenly. The solution was decanted into the separation funnel and slowly dropped into the potassium permanganate solution, then the drop-adding system was positioned on the magnetic stirrer in dark for 1 h. The accurate weighing 150 mg BSA was fully dissolved in carbonate buffer (pH = 9.6) to form BSA solution. The BSA solution was mixed with the above solution, and the pH was familiar to 10 with 1 mol/L sodium carbonate solution. Then, it was located on the magnetic stirrer and reacted in dark for 6 h. The reaction solution was added into the treated dialysis bag. Afterward, dialysis was finished in distilled water for 3 days, and replaced the dialysis solution twice a day. The solution in the dialysis bag was shifted to the freeze-dried bottle and the solution was prefrozen for 1–2 h at −20°C, followed by 48 h freeze-drying on the freeze-drying machine (LGJ-10, Beijing Yaxing Co., China). Finally, GL-BSA freeze-dried powder was acquired.

Preparation of glycyrrhizin-bovine serum albumin-luteolin nanoparticles of luteolin

GL-BSA-Lut-Nps were prepared by solvent removal method. Initially, GL-BSA freeze-dried powder of 8 mg was precisely weighed and added

to 1 mL carbonate buffer and mixed. Then, 3 mg Lut was liquefied in 1 mL ethanol, and the mixed Lut ethanol solution was added to 89 mL anhydrous ethanol for shaking and mixing. The ethanol solution was slowly added to the albumin carbonate system in accordance with 1 mL/min drop acceleration rate and 75 μL of 0.5% glutaraldehyde was rapidly added when the drop was completed for light-avoiding sealing and curing for 12 h. Finally, the solidified system was centrifuged (Zhongjia Co., China) at 13000 r/min for 20 min and the supernatant was prudently sucked away. The precipitate was dissolved in an appropriate amount of PBS, centrifuged at 8000 r/min for 20 min and the supernatant was absorbed and retained. The supernatant was firstly frozen for 1–2 h at −20°C, followed by freeze-dried for 48 h on a freeze-drying machine and finally, the GL-BSA-Lut-Nps freeze-dried powder was gotten. The experiment was performed according to Table 1.

Cell culture and inhibition screening of Bel-7402 cell activity by glycyrrhizin-coupled bovine serum albumin-loaded luteolin nanoparticles

Bel-7402 cells were cultured with 10% fetal bovine serum, 1 × 10 mg/L penicillin and 100 mg/L streptomycin in 37°C and 5% CO_2 (incubator MCO-15AC, SANYO Co., Japan). The digestion cells were subcultured by 0.25% trypsin. MTT assay was employed to perceive the proliferation inhibition of Bel-7402 cells. GL-BSA-Lut-Nps 0.375., 0.75, 1.25, 2.5, 5 mg/mL dose group, control group (DMEM high glucose medium containing 10% fetal bovine serum and 1% penicillin-streptomycin solution), Lut (100 μg/mL) group and 5-FU (52 μg/mL) positive group. The cells were cultured in 96-well cell culture plates and five replicate wells were finished in one group. After 24 h treatment, 10 μL MTT (5 mg/mL) was added to each well and incubated at 37°C for 4 h. After the supernatant was gradually detached, 150 mL of DMSO solution was added to each well and the culture plate was positioned horizontally on the shaking table. After slow shaking for 15 min, the absorbance value of each hole was noticed by selecting the channel with the wavelength of 490 nm on the enzyme labeling instrument (BIO-RAD, USA). The proliferation inhibition of five nanoparticles on Bel-7402 cells for 24 h was evaluated by the MTT method and the IC_{50} value was considered.

Solid characterization of glycyrrhizin-coupled bovine serum albumin-loaded luteolin nanoparticles

Differential scanning calorimetry analysis of glycyrrhizin-coupled bovine serum albumin-loaded luteolin nanoparticles (differential scanning calorimeter Detection)

Lut of 5 mg and lyophilized powder of 5 mg GL-BSA-Nps were truthfully weighed into a sample cell for differential scanning calorimetry analysis in the environment of pure nitrogen. The flow-through rate of nitrogen was 40 mL/min, and the temperature was augmented from room temperature to 350°C at a rate of 10°Caminutes.

Table 1: Experimental design factors

Factors	A (mg/mL)	B	C	D (mL/min)	E (μL)
1	2	9	1:6	1.5	75
2	8	10	1:6	0.5	50
3	4	8	1:9	1.5	25
4	8	7	1:9	1	75
5	8	10	1:6	0.5	50

The experiment included 5 factors: concentration of GL-BSA (A), influence of pH value of aqueous phase (B), volume ratio of aqueous phase to organic phase (C), droplet acceleration of anhydrous ethanol (D), and dosage of glutaraldehyde (E) of 0.5%; 5 levels were designed for each factor. GL-BSA: Glycyrrhizin-coupled Bovine Serum Albumin

Thermogravimetric analysis of glycyrrhizin-coupled bovine serum albumin-loaded luteolin nanoparticles (thermal gravimetric detection)

Precision respectively according to take 10 mg of Lut powder, bovine GL-BSA-Lut-Nps, producing samples in the sample pool, pure nitrogen gas environment under the condition of thermal gravimetric analysis (TGA) testing, testing conditions, N_2 20 mL/min, temperature from room temperature to 600°C, the heating rate is 10°C/min, record the weightlessness curve.

Solubility analysis of glycyrrhizin-coupled bovine serum albumin-loaded luteolin nanoparticles

The absorbance values of Lut and screening GL-BSA-Lut-Nps freeze-dried powder samples were evaluated by ultraviolet spectrophotometer (Yipu co., China).

Targeting effect of glycyrrhizin-coupled bovine serum albumin-loaded luteolin nanoparticles on Bel-7402 cells

We indeed weighed 7.56 g sodium bicarbonate, 1.06 g sodium carbonate and 7.36 g sodium chloride, added distilled water to 1 L and adjusted pH to 9 to prepare protein labeled crosslinking reaction solution. Then we exactly weighed 66.875 g ammonium chloride and added water to a constant volume of 0.25 L that is, a solution with a concentration of 5 mol/L and a pH of 8.5 was arranged to prepare the cross-linking termination solution. Finally, we formulate FITC 10 mg/mL solution. GL-BSA-Nps-FITC were prepared as follows, 1 mg of protein was dissolved in 0.5 mL of the crosslinking reaction solution and 15–20 times (number of molecules) of FITC was added to mix evenly and the reaction was conducted at 4°C overnight in the dark for more than 8 h. An appropriate amount of NH_4Cl solution of 5 mol/L was added until the final concentration was 50 mol/L and the reaction was terminated 2 h away from light at 4°C. Finally, the crosslinked products were dialyzed in PBS for more than 4 times until the dialysis solution was pure and then freeze-dried and stored away from light at 4°C.

Bel-7402, Hela and HCT8 cells were cultured from seed plate to six-well plates in a culture bottle. After the cells followed to the wall, GL-BSA-Nps-FITC was added to the culture solution group with FITC as the control well. The excitation wavelength in the range of 450–500 nm and emission wavelength in the range of 515–565 nm were nominated to show green fluorescence and the staining results were chronicled and snapped.

Detection of cell cycle and apoptosis

Cell cycle detection was achieved. GL-BSA-Lut-Nps-4, Lut, 5-Fu treated cells for 24 h, the cells were collected, adjusted to 10^6/mL, washed twice in PBS, centrifuged for 5 min at 250 r/min and the supernatant was detached as far as possible. The cells were fixed with 1 mL of precooled 70% ethanol at −20°C and added drop by drop, oscillating while adding, to confirm adequate fixation and stop cell agglomeration. The cells were fixed at 4°C for more than 30 min. Wash with PBS twice, centrifuge at 2000 r/min for 5 min and discard supernatant carefully to prevent cell loss. 500 μL propidium iodide was added and incubated at 37°C for 30 min. The cell cycle was perceived and analyzed by flow cytometry. Apoptosis detection was carried out. GL-BSA-Lut-Nps-4, Lut, 5-Fu cells were composed after 24 h. Add 5 μL FITC Annexin V and 10 μL PI, somewhat oscillate, incubate for 15 min at room temperature, add

300 μL Binding Buffer, use flow cytometry to notice the percentage of early apoptotic and middle-late apoptotic cells, and calculate the apoptosis rate.

Graph pad Prism 5.0 statistical analysis was pragmatic and the results were signified as mean ± standard deviation. $P < 0.05$ designated statistically significant differences.

1 hydrogen-nuclear magnetic resonance metabolomics analysis of glycyrrhizin-coupled bovine serum albumin-loaded luteolin nanoparticles-4 treated Bel-7402 cells

Preparation of cell metabolite samples

Add 5 mL 2–3 × 105 cells/mL Bel-7402 cell suspension to 50 cm^2 culture dishes for overnight culture. After cell adherence, GL-BSA-Lut-Nps-4 with concentrations of 0.375, 0.75, 1.25, 2.5, 5 mg/mL was added and cultured for 24 h. The negative control group was only cultured in DMEM, while the positive control groups were added with Lut and 5-FU, respectively. The cells were scraped from the petri dish, then centrifuged for 5 min at 4°C for 1000 r/min, washed with PBS for two times and the precipitation was composed. The intracellular metabolites were extracted by methanol-chloroform and ultrapure water biphase extraction,[25,26] dried with nitrogen blower and stored in the refrigerator at −80°C. 350 mL of tsp-containing heavy water and 0.1 mol/L PBS (pH = 7.4) were added to the cell extracts, centrifuged at 4°C for 10 min at 13,000 r/min and the supernatant was verified in a 5 mm nuclear magnetic resonance (NMR) tube.

1 hydrogen-nuclear magnetic resonance determination and spectra processing

The 1 hydrogen-NMR (^{1}H NMR) spectra were composed with Bruker AVANCE III, 500MHz nuclear magnetic resonance instrument (Bruker, Switzerland). The pulse sequence of Carr-Purcell-Mei boom-Gill (recycle delay-90° (τ-180°-τ) n-acquisition was employed, in which accumulation times was 512 and acquisition points was 32 k, delay time was set to be 3 s and spectral width was 10 kHz. Free induction decay signals are transformed to NMR spectra by 32 k Fourier transform. After the peak phase and baseline correction, the peak integrals (δ0.50–9.00) were intended with Topspin (Version 2.1, Bruker Biospin) software with the integral interval of 0.004 ppm. The integral intervals at δ4.70–5.20 were set to be zero to eradicate the impact of the water peak. The integral was regularized to the sum of the integrals in a whole spectrum and these data were employed for Principal Component Analysis (PCA) with SIMCA-P^+ 12.0 software (Umetrics, Sweden). Scores plot was employed to signify the analysis results in PCA. The scores plot can visually imitate the spatial distribution of each sample.

RESULTS

Cell survival rate test and glycyrrhizin-coupled bovine serum albumin-loaded luteolin nanoparticles screening

In this experiment, Bel-7402 cells were cultured and the antitumor effect of artificial modified GL-BSA-Lut-Nps *in vitro* was considered by MTT assay. The survival rate of Bel-7402 cells cultured on 96 well plates for 24, 48, and 72 h was perceived. Our research group found that the effect of nanoparticles on tumor cell proliferation was sturdiest at 24 h. It may be due to the abrupt release of nano-drugs, which leads to the peak release of drugs at 24 h and after 72 h of intervention, the state of cells is poor. Considering the possible factors, our research group designated five parallel prescription samples of GL-BSA-Lut-Nps for the MTT experiment, focusing on the cell survival rate of cultured Bel-7402 cells for 24 h and the preliminary evaluation of the efficacy stability under the preparation conditions. As shown in Table 2 and Figure 1, the survival rate of Bel-7402 cells lessened gradually with the increase of GL-BSA-Lut-Nps dose, showing a dose-effect relationship. In the MTT experiment, the concentration of 5-FU was 100 μg/mL and the Lut was 52 μg/mL. After calculation, the total amount of Lut controlled in the 5 mg/mL concentration of the Nps was basically the same as the concentration of Lut in the cell fluid, so the comparison disclosed that the inhibitory effect of nanoparticles on Bel-7402 proliferation was stronger than that of Lut. The cell survival rate was premeditated by SPSS statistical software to obtain the IC_{50} value. After 24 h of intervention, the IC_{50} values of the five drugs were 10.730 ± 1.120, 6.079 ± 0.580, 3.602 ± 1.220, 1.999 ± 0.880 and 3.443 ± 0.990 mg/mL, respectively. Finally, sample No. 4 had the finest anti-tumor cell effect *in vitro*. The experimental data and statistical images are provided in Table 2 and Figure 1.

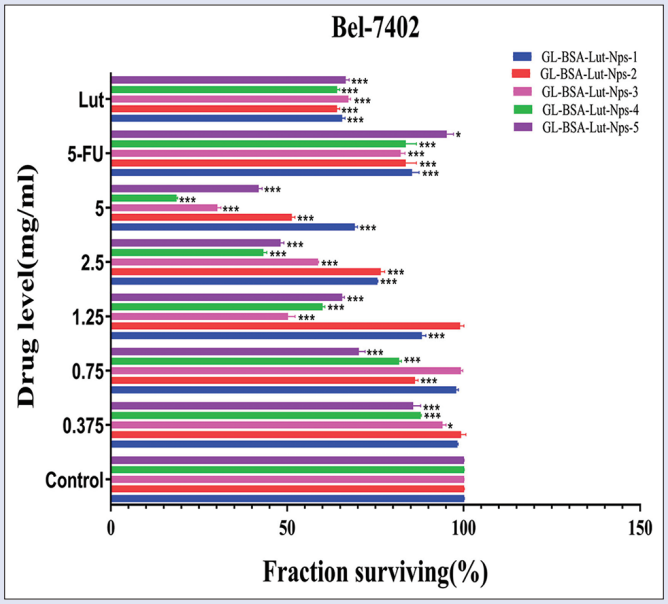

Figure 1: 3-(4,5-dimethyl-2-thiazolyl)-2,5-diphenyl-tetrazolium bromide experimental cell survival rate test. The cell survival rate shows mean ± standard deviation ($n = 3$); *$P < 0.05$, **$P < 0.01$, ***$P < 0.001$, versus respective controls analyzed

Determination of particle size of glycyrrhizin-coupled bovine serum albumin-loaded luteolin nanoparticles-4

The particle size of GL-BSA-Lut-Nps-4 was distinguished by nanometer (Nano S90, Malvern Co., Britain) after complex dissolution and the image data are exposed in Figure 2a. The particle size of GL-BSA-Lut-Nps is distributed between 70 nm and 550 nm, but it is mainly distributed between 200 and 300 nm [Figure 2a]. The Polymer Dispersity Index of No. 4 prescription sample is 0.737 and the average particle size is 225.3 ± 7.2 nm.

Table 2: Inhibitory effect of five prescriptions of Glycyrrhizin-coupled Bovine Serum Albumin-Lut-Nps on the proliferation of Human HCC line Bel-7402 ($\bar{x}$±standard deviation)

Drug level (mg/mL)	24 h cell survival rate (%)				
	1	2	3	4	5
Control	100.10±0.08	100.10±0.09	100.10±0.02	100.10±0.04	100.10±0.03
0.375	98.22±0.22	99.26±1.39	94.00±1.01*	87.80±0.21***	85.70±2.11***
0.75	97.86±0.65	86.20±0.88***	99.20±0.56	81.70±0.66***	70.30±1.76***
1.250	88.12±1.16***	99.00±1.07	50.20±2.01***	60.00±0.68***	65.60±0.64***
2.5	75.52±0.17***	76.50±1.12***	58.70±0.22***	43.20±1.03***	48.10±0.95***
5	69.11±0.77***	51.30±0.86***	30.20±1.03***	18.60±0.33***	41.90±0.98***
5-Fu	85.33±2.02***	83.58±3.01***	82.11±1.25***	83.58±3.01***	95.20±1.90*
Lut	65.53±0.84***	64.11±0.76***	67.30±0.66***	64.11±0.76***	66.59±0.95***

Compared with control, *P<0.05, **P<0.01, *** P<0.001

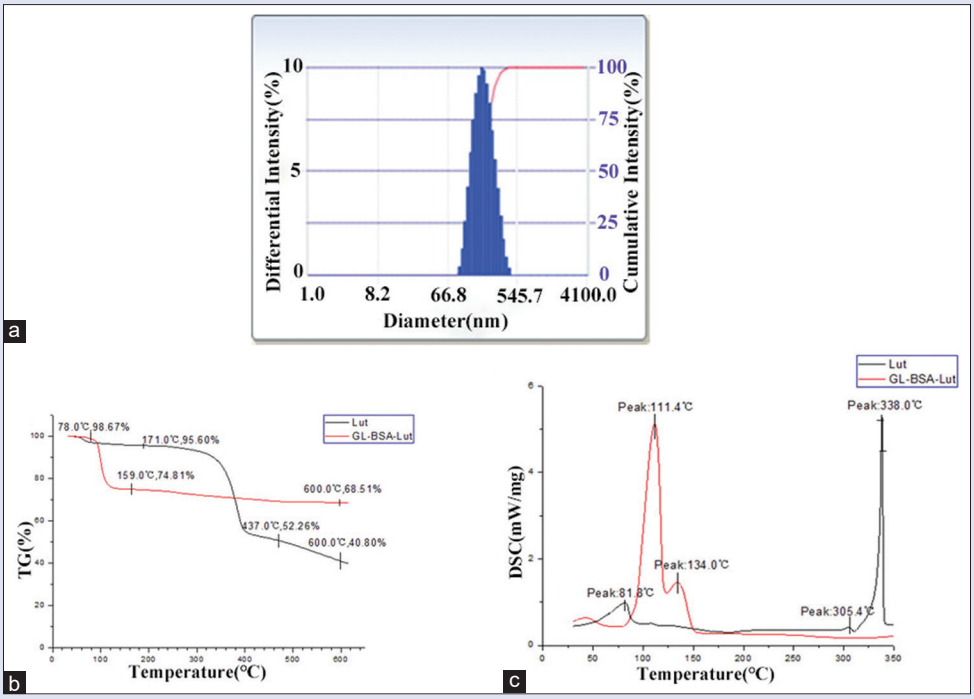

Figure 2: (a) Particle size distribution of glycyrrhizin-coupled bovine serum albumin-loaded luteolin nanoparticles; (b) The rmogravimetric analysis of glycyrrhizin-coupled bovine serum albumin-loaded luteolin nanoparticles-4; (c) Differential thermal scanning pattern of the glycyrrhizin-coupled bovine serum albumin-loaded luteolin nanoparticles-4

Thermal gravimetric analysis of glycyrrhizin-coupled bovine serum albumin-loaded luteolin nanoparticles-4 (thermal gravimetric detection)

Thermal gravimetric (TG) test results [Figure 2b] revealed that Lut lost weight in the range of 30°C–78°C, which may be correlated to the evaporation of water in the crystal water contained in Lut itself. When the temperature rose to about 300°C, Lut lost weight again. The GL-BSA-Lut-Nps-4 curve showed that when the temperature augmented to about 100°C, there was momentous weightlessness, with a weightlessness rate of 25%, this was due to the evaporation of water in the freeze-dried nanopowder and the temperature was enlarged to 600°C, the weightlessness of the whole nano system was not understandable. TG detection indicated that the vast majority of Lut was fruitfully encapsulated by nano carrier. The structure is steady, which is dependable with the above Differential scanning calorimeter (DSC) results.

Differential scanning calorimetry analysis of glycyrrhizin-coupled bovine serum albumin-loaded luteolin nanoparticles-4 (differential scanning calorimeter detection)

In the test results [Figure 2c], Lut curve specified that Lut had a significant heat absorption peak at the dab of 338.0°C, a weaker heat absorption peak at dab of 81.8°C and 305.4°C dab, demonstrating that Lut powder had crystalline morphology. GL-BSA-Lut-Nps-4 in 111.4°C has a foremost heat absorption peak that may be only a small amount of Lut adhered to the surface of the nanoparticle, in addition to this there is no palpable heat absorption peak showing that GL-BSA-Lut-Nps-4 is functional, and the package of Lut was typically limited.

Aqueous solubility analysis of glycyrrhizin-coupled bovine serum albumin-loaded luteolin nanoparticles-4

The maximum absorption wavelength of GL-BSA-Lut-Nps-4 and Lut was 339 nm by spectral scanning with UV-visible spectrophotometer. Standard solutions with different concentrations were constructed and the standard solutions were evaluated with UV-visible spectrophotometer at 339 nm and the test grades are shown in Tables 3 and 4.

It can be seen from Figure 3 that when the Lut powder is liquefied in water, the aqueous solution is yellow and turbid and there is a large amount of precipitate after standing. However, GL-BSA-Lut-Nps-4 dissolved quickly and did not precipitate after standing and the solution was yellowish and transparent. According to the results of Figure 3 and Tables 3 and 4, the solubility of Lut in water is tremendously low. Its aqueous solubility value is 1.7×10^{-5} g/mL and the aqueous solubility of GL-BSA-Lut-Nps-4 is very high, with its solubility value being 1.5×10^{-2} g/mL. The aqueous solubility of GL-BSA-Lut-Nps-4 is more than 1000 times higher than that of Lut powder, which further illustrations the nanoparticles preparation advantages and application prospects of the modification.

Table 3: Optical density values of Glycyrrhizin-coupled Bovine Serum Albumin-Lut-Nps-4 aqueous solution

Drug level (PPM)	OD			Average value
	1	2	3	
4000	0.195	0.199	0.197	0.197
3000	0.141	0.142	0.143	0.142
2000	0.099	0.097	0.096	0.097
1000	0.048	0.048	0.049	0.048
500	0.020	0.020	0.019	0.020
Saturated aqueous solution/2	0.749	0.749	0.749	0.749

OD: Optical density

Table 4: Optical density values of Luteolin aqueous solution

Drug level (PPM)	OD			Average value
	1	2	3	
10	0.380	0.379	0.382	0.380
7.5	0.367	0.375	0.374	0.372
5	0.198	0.199	0.199	0.199
2.5	0.104	0.105	0.108	0.106
1.25	0.115	0.117	0.113	0.115
Saturated aqueous solution	0.653	0.666	0.667	0.662

OD: Optical density

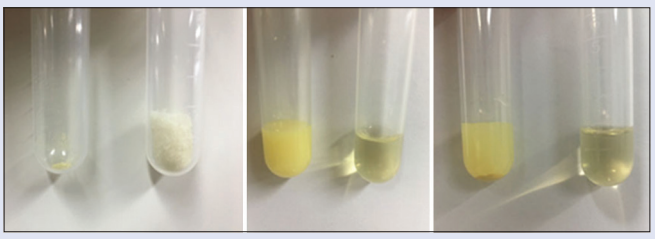

Figure 3: Dissolve Before (left), after (middle) and after standing the image (right) dissolution of luteolin and glycyrrhizin-coupled bovine serum albumin-loaded luteolin nanoparticles-4

Fluorescein isothiocyanate fluorescence staining analysis of three cell lines administered with glycyrrhizin-coupled bovine serum albumin-loaded luteolin nanoparticles-4

In the experiment, FITC was coupled with GL-BSA-Lut-Nps to obtain GL-BSA-Lut-Nps-FITC labeled drugs. Bel-7402, Hela, and HCT8 cells were treated with labeled drugs for 24 h and detected under the fluorescence microscope. As shown in Figure 4, the fluorescence images of the FITC control group and GL-BSA-Lut-Nps-4-FITC treatment group were evidently noticeable. There was no noteworthy difference in fluorescence intensity between the HCT8 cells and the control group. In Hela and Bel-7402 cells, the fluorescence intensity and quantity of the drug group were higher than those of the control group, and the difference between Bel-7402 cells was the most substantial. This submits that GL-BSA-Lut-Nps-4 has a targeting effect on the Bel-7402 cells after acting on tumor cells and GL-BSA-Lut-Nps-4 has the hepatic inclination.

Detection of cell cycle and apoptosis on glycyrrhizin-coupled bovine serum albumin-loaded luteolin nanoparticles-4

In cell cycle and apoptosis recognition, the control, Lut, positive 5-FU and drug groups were set up. Figure 5a demonstrates that compared with the control group, GL-BSA-Lut-Nps-4, Lut and 5-FU showed a convinced inhibitory effect on cell cycle. The Nps-4 showed obvious S phase block in a dose-dependent manner. The G1 phase block of 5-FU group was sturdy, but S phase block was weaker than the Nps-4 and the Lut and the Nps-4 has better cycle blocking effect than that of the Lut. These results imitate that Nps-4 does have good antitumor effect, which is also the implication of this study. It is showed that Nps-4 could inhibit tumor proliferation by blocking S progression of the Bel-7402 cell cycle.

After 24 h of Bel-7402 cells treated with different experimental group, the apoptosis rate in each group was sensed by Annexin V-FITC/PI assay. In Figure 5b, the apoptosis rate of Bel-7402 cells in the GL-BSA-Lut-Nps-4 group was the uppermost (65.70%), and the apoptosis rate of Lut group (35.93%) was similar to that of the 5-Fu group (29.70%), which was higher than that of control group (22.98%). The results specified that the effect of GL-BSA-Lut-Nps-4 group on inducing tumor cell apoptosis

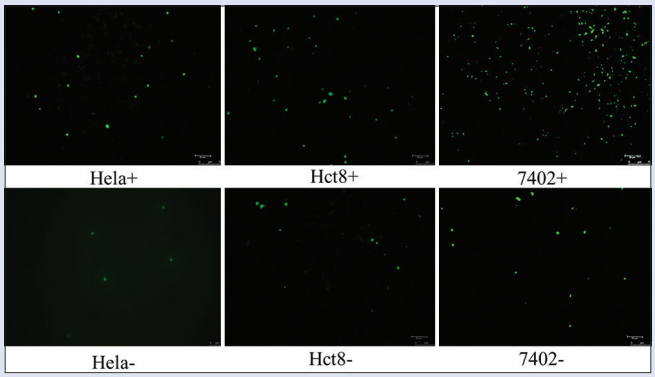

Figure 4: Staining diagram of three cell lines treated with fluorescein isothiocyanate fluorescent labeled glycyrrhizin-coupled bovine serum albumin-loaded luteolin nanoparticles-4 ("+" means administration,"–"means control)

Table 5: Main metabolites of bel-7402 cells 24 h after treated

Peak number	Metabolites	δ¹H (ppm)	Perssad
1	2-oxyleucine	0.92 (d)	CH_3, CH_2
2	Isoleucine	0.93 (t), 1.01 (d)	δ-CH_3, δ′-CH3δCH_3, γ-CH_3
3	Leucine	0.97 (t), 0.99 (d)	CH=CH
4	Valine	1.01 (d,), 1.04 (d,)	γ-CH_3, γ′-CH_3
5	3-hydroxybutyrate	1.18 (d)	γ-CH_3
6	Lactate	1.33 (d), 4.12 (q)	α-CH, β-CH_3
7	Alanine	1.48 (d), 3.78 (d)	β-CH_3
8	Acetate	1.92 (s)	CH_3
9	Glutamate	2.09 (m), 2.35 (m) 3.78 (m)	α-CH, β-CH_2, γ-CH_2
10	Glutamine	2.15 (m), 2.46 (m), 3.78 (m)	α-CH, β-CH_2, γ-CH_2
11	Dimethylamine	2.73 (s)	CH_3
12	Trimethylamine	2.91 (s)	CH_3
13	Asparagine	2.82 (dd)	CH_3
14	Tyrosine	3.19 (dd) 6.91 (d), 7.19 (d)	3 or 5-CH, 2 or 6-CH
15	Choline	3.20 (s)	N $(CH_3)_3$
16	Arginine	3.22 (m)	$(NH_2)_2C(=NH)$
17	TMAO	3.27 (s)	N $(CH_3)_3$
18	Glucose	3.30–3.90	CH
19	Taurine	3.25 (t) 3.43 (t)	CH_2SO_3, NCH_2
20	Threonine	3.59 (d)	$(NH_2)_2C(=NH)$
21	Glycerol	3.56 (dd), 3.66 (dd)	CH
22	α-glucose	5.23 (d)	β-CH_2, β′-CH_2
23	β-glucose	4.65 (d)	CH
24	Creatine	3.93 (s)	β-C1H
25	1-methylhistidine	7.22 (s)	5-CH,1,3-CH_3,4,6-CH,2-CH
26	Phenylalanine	7.33 (m), 7.38 (m), 7.43 (m)	2-CH, 4-CH, 3-CH
27	Uridine	7.88 (d)	C_1=NC=NC=C_1
28	Histidine	7.09 (s), 7.38 (s)	5-CH, 3-CH
29	Formate	8.46 (s)	CH

s: Singlet, d: Doublet, dd: Doublet of doublet, t: Triplet, m: Multiple

was stronger than that of Lut and 5-FU, which also discovered one of the reasons for the improved effect of anti-tumor cell proliferation after the construction of nanoparticles.

1 hydrogen-nuclear magnetic resonance spectra analysis of the cells

^{1}H NMR spectra of cells are presented in Figure 6. Combined with relevant literatures and preceding studies,[27,28] the metabolites in the spectra were allocated. We can see that metabolites are connected to lipid, amino acid, and carbohydrate metabolism [Table 5].

Multivariate data analysis of cellular metabolites

After normalization of the blank control group and GL-BSA-Lut-Nps treatment group, the integral area was analyzed by SIMCA-P+12.0 software (Umetircs, Sweden). After treatment with GL-BSA-Lut-Nps, cellular metabolites diminished lactate, 3-hydroxybutyrate, lipid, tyrosine, and β-glucose compared to the control group, while glutamate, asparagine, choline, and creatine augmented. The scores plot of PCA is given in Figure 7. As can be seen from the figure, after 24 h of administration, there was a noteworthy difference between the blank control group and the GL-BSA-Lut-Nps-4-treated group, while the Lut-treated group and the 5-FU-treated group were positioned between the two groups. The four groups showed an obvious tendency, which publicized that there are many metabolic variations in treated groups and the effect of GL-BSA-Lut-Nps-4 treatment is inordinate.

DISCUSSION

In this experiment, five GL-BSA-Lut nanoparticles were arranged by solvent removal method. The 24 h anti-cancer cells activity of the five nanoparticles was partitioned by MTT assay. The IC_{50} value presented that GL-BSA-Lut-Nps-4 had the strongest inhibitory effect on Bel-7402 cells. The earlier study of the research group showed that the largest encapsulation efficiency of nanoparticles is 30.33%.[23] Based on the 24 h MTT IC_{50} results, the drug loading capacity of GL-BSA-Lut-Nps-4 was 23.988 μg/mL. Compared with the actual dose of Lut IC_{50} which was 52.940 μg/mL, the efficacy of GL-BSA-Lut-Nps-4 was suggestively better than that of the Lut. At present, there is a gap in the identification of the created Lut carrier nanoparticles and their structures at home and abroad. We want to conduct preliminary structural and performance identification of the screened GL-BSA-Lut-Nps-4 to plug these gaps on the one hand and authorize the reliability of the source of Lut nanoparticles on the other hand.

The smaller the nanoparticles, the greater the potential drug application value the more the drug-loading NPs deposit in tumor tissues, the more they can infiltrate the vascular wall space of tumor tissues and the more clear the anti-tumor effect will be. The average particle size of No. 4 was 225.3 ± 7.2 nm. However, we can additionally study the morphology of nanoparticles, which is one of the research directions of the follow-up research group.

Differential scanning calorimetry (DSC) is a method to measure the correlation between time (or temperature) and the temperature difference between a sample and the reference material under the condition that the programmed temperature is relentless or variable.[29] TG is a technical way to study the correlation between the mass change of a substance and time (or temperature).[30] These two methods were largely employed to classify the authenticity of Chinese medicinal materials compositions.[31] In this experiment, DSC and TG results showed that Lut was effectively wrapped by GL-BSA-Nps. The feasibility and superiority of the experimental prescription were further elucidated. From the results of the FITC targeting test, we know that there is a

positive degree of fluorescence intensity and surge in the number of nanoparticles for liver cancer cells, signifying that GL-BSA-Lut-Nps-4 have a higher affinity to liver cancer cells and shimmering its good targeting. Glycyrrhizic acid receptors occur on the surface of hepatocytes, so the drug coupled with glycyrrhizic acid can rise the active targeting of drugs to the liver.

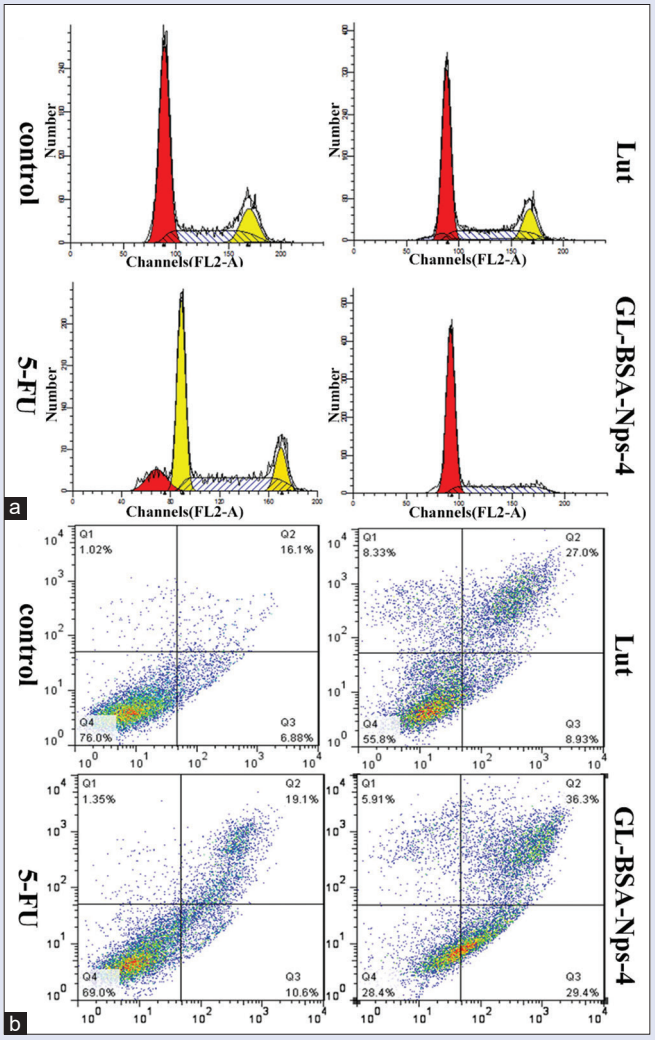

Figure 5: (a) Cell cycle detection based on four experimental groups of Bel-7402 cells (b) Annexin v-fluorescein isothiocyanate/propidium iodide assay was used to detect apoptosis in four experimental groups of Bel-7402 cells

The study of the inhibitory effect of drugs on the tumor cell cycle is supportive for us to understand the molecular mechanism of drug suppress proliferation of cancer cells. In this study, we considered the effects of GL-BSA-Lut-Nps-4 and Lut on the cell cycle of Bel-7402 and the fallouts showed that GL-BSA-Lut-Nps-4 significantly jammed the S-phase progression of tumor cells Bel-7402 and the blocking effect was stronger than that of Lut at the same dose. Our results are reliable with the results of other drugs blocking other tumor cell cycles in the literature.[32-34] The Annexin V-FITC/PI double staining method was employed to perceive the ability of GL-BSA-Lut-Nps-4 to induce apoptosis of Bel-7402 cells. The results of flow displayed that the apoptosis rate of GL-BSA-Lut-Nps-4 group was the maximum and the apoptosis rate of Lut and 5-FU was similar, but visibly diminished when compared with the GL-BSA-Lut-Nps-4. The results show that GL-BSA-Lut-Nps-4 could ominously induce apoptosis of Bel-7402 cells and the effect was better than that of Lut and 5-FU positive control, which was steady with the results of previous MTT and cell cycle experiments. Cell cycle and apoptosis results evidently explicated the reasons for the good anti-tumor proliferation of GL-BSA-Lut-Nps-4 cells and showed superior effect compared with Lut, which was reliable with the purpose and significance of constructing nanoparticles.

GL-BSA-Lut-Nps-4 can control the metabolism of liver cancer Bel-7402 cells. It can regulate aerobic oxidation, phospholipid metabolism, energy metabolism, amino acid metabolism and so on.[35] Amino acids are the most rudimentary substances in life activities. The growth of tumor cells requires a large amount of amino acids. Studies have publicized that tumors can lead to amino acid metabolism illnesses.[36] Chen *et al.* proposed that miR-3662 can inhibit glycolysis by dipping lactic acid production, glucose consumption, cell glucose 6-phosphoric acid level, ATP production, extracellular acidification rate, and snowballing oxygen consumption rate in HCC.[37] The results showed that the content of lactic acid reduced after administration, which specified that nanoparticles could inhibit the growth of HCC cells. Glutamine is one of the energy sources of tumor cells and its metabolism produces glutamic acid and glutathione. Leucine, isoleucine and valine, which are connected to the biosynthesis and degradation of proteins, are vital amino acids *in vivo.* Among them, the branch chain amino acid isoleucine augmented in HCC, while

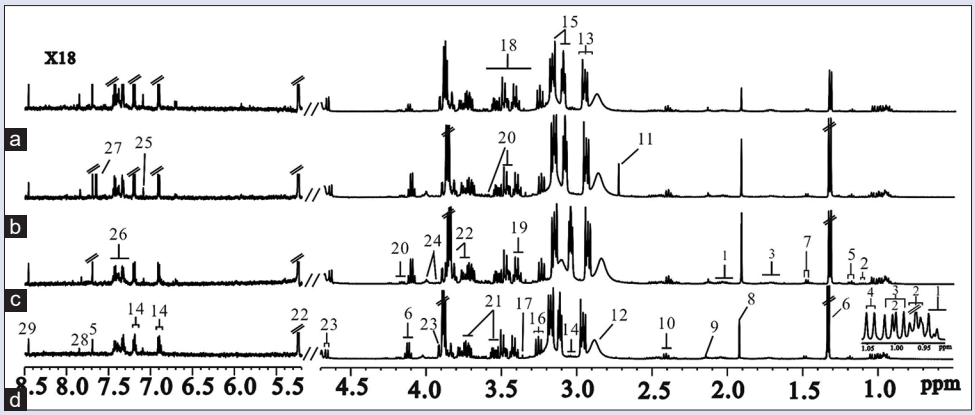

Figure 6: 1 hydrogen-nuclear magnetic resonance spectra of cells in each group after 24 h administration (a) 5-Fluorouracil-treated (b) Lut-treated (c) luteolin-glycyrrhizin-coupled bovine serum albumin-nanoparticle-treated (d) controls

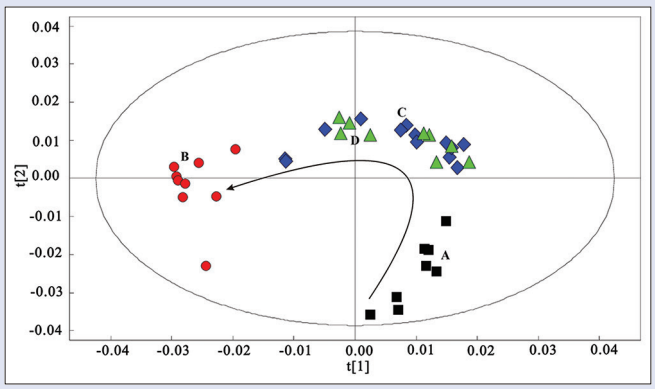

Figure 7: Scores plot of the four kinds of cells ($R^2X = 92.8\%$, $Q^2 = 71.4\%$) (A) Controls, (B) glycyrrhizin-coupled bovine serum albumin-loaded luteolin nanoparticles-4-treated, (C) Lut-treated, (D) 5-FU-treated

glutamic acid diminished in HCC. In mouse models of liver cancer, lipid histology and metabolomics analysis showed that liver mTORC2 promoted *ab initio* fatty acid and lipid synthesis, leading to steatosis and tumor development. In the experiment, the reduction of lipids also better recommends that drug-loaded nanoparticles inhibit the growth of liver cancer.

CONCLUSION

In this experiment, five kinds of GL-BSA-Lut-Nps were organized and curtained for their anti-tumor cells activity and the most active nanoparticles were acquired. The particle size, structure characterization, and solubility of GL-BSA-Lut-Nps-4 were spotted and the results of cycle and apoptosis delivered evidence that GL-BSA-Lut-Nps-4 could inhibit the growth of liver cancer Bel-7402 cells. The study of cell metabolomics further exposed that GL-BSA-Lut-Nps-4 could inhibit the proliferation of Bel-7402 cells and knowingly regulate the amount of differential metabolites in Bel-7402 cells, thus refining the metabolic disorder of Bel-7402 cells. The feasibility and superiority of the GL-BSA-Lut-Nps-4 preparation created have been proved, which also offers the method and basis for the Lut formulation and the research on anti-tumor drugs treatment of liver cancer.

Financial support and sponsorship

This work was supported by the National Natural Science Foundation of China (No. 22074024, 81102753), Key scientific research platforms and projects of Guangdong colleges and universities (No. 2021ZDZX2043), Natural Science Foundation of Guangdong Province (No. 2214050009294), and Guangdong Science and Technology Innovation Strategy Special Program projects (No. 2019A1515011726).

Conflicts of interest

There are no conflicts of interest.

REFERENCES

1. Chen W, Sun K, Zheng R, Zeng H, Zhang S, Xia C, *et al.* Cancer incidence and mortality in China, 2014. Chin J Cancer Res 2018;30:1-12.
2. Valery PC, Laversanne M, Clark PJ, Petrick JL, McGlynn KA, Bray F. Projections of primary liver cancer to 2030 in 30 countries worldwide. Hepatology 2018;67:600-11.
3. Chen W. Cancer statistics: Updated cancer burden in China. Chin J Cancer Res 2015;27:1.
4. Bosch FX, Ribes J, Díaz M, Cléries R. Primary liver cancer: Worldwide incidence and trends. Gastroenterology 2004;127 Suppl 1:S5-16.
5. Chen W, Zheng R, Baade PD, Zhang S, Zeng H, Bray F, *et al.* Cancer statistics in China, 2015. CA Cancer J Clin 2016;66:115-32.
6. Nguyen VT, Law MG, Dore GJ. Hepatitis B-related hepatocellular carcinoma: Epidemiological characteristics and disease burden. J Viral Hepat 2009;16:453-63.
7. Kumar S, Pandey AK. Chemistry and biological activities of flavonoids: An overview. ScientificWorldJournal 2013;2013:162750.
8. Huang X, Dai S, Dai J, Xiao Y, Bai Y, Chen B, *et al.* Luteolin decreases invasiveness, deactivates STAT3 signaling, and reverses interleukin-6 induced epithelial-mesenchymal transition and matrix metalloproteinase secretion of pancreatic cancer cells. Onco Targets Ther 2015;8:2989-3001.
9. Han K, Meng W, Zhang JJ, Zhou Y, Wang YL, Su Y, *et al.* Luteolin inhibited proliferation and induced apoptosis of prostate cancer cells through miR-301. Onco Targets Ther 2016;9:3085-94.
10. Naso LG, Badiola I, Marquez Clavijo J, Valcarcel M, Salado C, Ferrer EG, *et al.* Inhibition of the metastatic progression of breast and colorectal cancer *in vitro* and *in vivo* in murine model by the oxidovanadium (IV) complex with luteolin. Bioorg Med Chem 2016;24:6004-11.
11. Al-Megrin WA, Alkhuriji AF, Yousef AO, Metwally DM, Habotta OA, Kassab RB, *et al.* Antagonistic efficacy of luteolin against lead acetate exposure-associated with hepatotoxicity is mediated via antioxidant, anti-inflammatory, and anti-apoptotic activities. Antioxidants (Basel) 2019;9:E10.
12. Aziz N, Kim MY, Cho JY. Anti-inflammatory effects of luteolin: A review of *in vitro*, *in vivo*, and *in silico* studies. J Ethnopharmacol 2018;225:342-58.
13. Tuorkey MJ. Molecular targets of luteolin in cancer. Eur J Cancer Prev 2016;25:65-76.
14. Zheng S, Cheng Y, Teng Y, Liu X, Yu T, Wang Y, *et al.* Application of luteolin nanomicelles anti-glioma effect with improvement *in vitro* and *in vivo*. Oncotarget 2017;8:61146-62.
15. Chakrabarti M, Ray SK. Anti-tumor activities of luteolin and silibinin in glioblastoma cells: Overexpression of miR-7-1-3p augmented luteolin and silibinin to inhibit autophagy and induce apoptosis in glioblastoma *in vivo*. Apoptosis 2016;21:312-28.
16. Imran M, Rauf A, Abu-Izneid T, Nadeem M, Shariati MA, Khan IA, *et al.* Luteolin, a flavonoid, as an anticancer agent: A review. Biomed Pharmacother 2019;112:108612.
17. Simard JR, Zunszain PA, Ha CE, Yang JS, Bhagavan NV, Petitpas I, *et al.* Locating high-affinity fatty acid-binding sites on albumin by x-ray crystallography and NMR spectroscopy. Proc Natl Acad Sci U S A 2005;102:17958-63.
18. Langer K, Balthasar S, Vogel V, Dinauer N, von Briesen H, Schubert D. Optimization of the preparation process for human serum albumin (HSA) nanoparticles. Int J Pharm 2003;257:169-80.
19. Wang L, Zhong C, Zu Y, Zhao X, Deng Y, Wu W, *et al.* Preparation and characterization of luteolin nanoparticles for enhance bioavailability and inhibit liver microsomal peroxidation in rats. J Funct Foods 2019;55:57-64.
20. Peters T Jr. Serum albumin. Adv Protein Chem 1985;37:161-245.
21. Osaka S, Tsuji H, Kiwada H. Uptake of liposomes surface-modified with glycyrrhizin by primary cultured rat hepatocytes. Biol Pharm Bull 1994;17:940-3.
22. Kronemann N, Nockher WA, Busse R, Schini-Kerth VB. Growth-inhibitory effect of cyclic GMP- and cyclic AMP-dependent vasodilators on rat vascular smooth muscle cells: Effect on cell cycle and cyclin expression. Br J Pharmacol 1999;126:349-57.
23. Fu W, Chai D, Wen Y, Shijie W, Baoyun Y, Shaolian C, *et al.* Preparation of glycyrrhizin-coupled bovine serum albumin containing luteolin nanoparticles and their activity *in vitro*. J Trop Med 2018;18:22-7.
24. Cao Z, Zhang H, Cai X, Fang W, Chai D, Wen Y, *et al.* Luteolin promotes cell apoptosis by inducing autophagy in hepatocellular carcinoma. Cell Physiol Biochem 2017;43:1803-12.
25. Cuperlovic-Culf M, Cormier K, Touaibia M, Reyjal J, Robichaud S, Belbraouet M, *et al.* (1) H NMR metabolomics analysis of renal cell carcinoma cells: Effect of VHL inactivation on metabolism. Int J Cancer 2016;138:2439-49.
26. Teng Q, Huang W, Collette TW, Ekman DR, Tan C. A direct cell quenching method for cell-culture based metabolomics. Metabolomics 2009;5:199-208.
27. Wei L, Liao P, Wu H, Li X, Pei F, Li W, *et al.* Metabolic profiling studies on the toxicological effects of realgar in rats by 1H NMR spectroscopy. Toxicol Appl Pharmacol 2009;234:314-25.
28. Schepkens C, Dallons M, Dehairs J, Talebi A, Jeandriens J, Drossart LM, *et al.* A new classification method of metastatic cancers using a ^{1}H-NMR-based approach: A study case of melanoma, breast, and prostate cancer cell lines. Metabolites 2019;9:E281.
29. Demetzos C. Differential scanning calorimetry (DSC): A tool to study the thermal behavior of lipid bilayers and liposomal stability. J Liposome Res 2008;18:159-73.

30. Yu J, Wang P, Ni F, Cizdziel J, Wu D, Zhao Q, *et al.* Characterization of microplastics in environment by thermal gravimetric analysis coupled with Fourier transform infrared spectroscopy. Mar Pollut Bull 2019;145:153-60.
31. Boguta P, Sokołowska Z, Skic K. Use of thermal analysis coupled with differential scanning calorimetry, quadrupole mass spectrometry and infrared spectroscopy (TG-DSC-QMS-FTIR) to monitor chemical properties and thermal stability of fulvic and humic acids. PLoS One 2017;12:e0189653.
32. Hao G, Zhai J, Jiang H, Zhang Y, Wu M, Qiu Y, *et al.* Acetylshikonin induces apoptosis of human leukemia cell line K562 by inducing S phase cell cycle arrest, modulating ROS accumulation, depleting Bcr-Abl and blocking NF-κB signaling. Biomed Pharmacother 2020;122:109677.
33. Huang HH, Liu FB, Ruan Z, Zheng J, Su YJ, Wang J. Tetramethylpyrazine (TMPZ) triggers S-phase arrest and mitochondria-dependent apoptosis in lung cancer cells. Neoplasma 2018;65:367-75.
34. Kellum JA, Chawla LS. Cell-cycle arrest and acute kidney injury: The light and the dark sides. Nephrol Dial Transplant 2016;31:16-22.
35. Yang Y, Li C, Nie X, Feng X, Chen W, Yue Y, *et al.* Metabonomic studies of human hepatocellular carcinoma using high-resolution magic-angle spinning 1H NMR spectroscopy in conjunction with multivariate data analysis. J Proteome Res 2007;6:2605-14.
36. Li ZF, Wang J, Huang C, Zhang S, Yang J, Jiang A, *et al.* Gas chromatography/time-of-flight mass spectrometry-based metabonomics of hepatocarcinoma in rats with lung metastasis: Elucidation of the metabolic characteristics of hepatocarcinoma at formation and metastasis. Rapid Commun Mass Spectrom 2010;24:2765-75.
37. Chen Z, Zuo X, Zhang Y, Han G, Zhang L, Wu J, *et al.* MiR-3662 suppresses hepatocellular carcinoma growth through inhibition of HIF-1α-mediated Warburg effect. Cell Death Dis 2018;9:549.